

Asymmetry of Nonlinear Transport and Electron Interactions in Quantum Dots

D. M. Zumbühl and C. M. Marcus

Department of Physics, Harvard University, Cambridge, Massachusetts 02138

M. P. Hanson and A. C. Gossard

Materials Department, University of California, Santa Barbara, California 93106

(Dated: August 31, 2018)

The symmetry properties of transport beyond the linear regime in chaotic quantum dots are investigated experimentally. A component of differential conductance that is antisymmetric in both applied source-drain bias V and magnetic field B , absent in linear transport, is found to exhibit mesoscopic fluctuations around a zero average. Typical values of this component allow a measurement of the electron interaction strength.

Quantum transport in disordered mesoscopic conductors and chaotic quantum dots has been widely studied in the regime of linear response, and is well understood in terms of universal statistical theories [1], even in the presence of significant electron interaction [2, 3]. A central principle of linear mesoscopic transport concerns the symmetry of magnetoconductance: as a consequence of time reversal symmetry and microscopic reversibility close to equilibrium, the differential conductance $g = dI/dV$ of a two-terminal sample is symmetric in magnetic field B : $g(B) = g(-B)$ [4, 5, 6], with generalized reciprocity (Landauer-Büttiker) relations for multi-terminal coherent conductors [6]. Beyond linear response, i.e., at sufficient applied bias that the current I is no longer proportional to source-drain voltage V , these symmetry relations break down. Unless disallowed by some special symmetry, differential conductance beyond linear response can generally contain a component (here denoted \tilde{g}) that is proportional to both B and V :

$$\tilde{g} = \alpha VB. \quad (1)$$

For instance, contributions to g of the form in Eq. 1 are permitted in non-centrosymmetric materials [7], chiral conductors [8], including carbon nanotubes [9], or conductors with crossed electric and magnetic fields [10].

In the absence of electron interaction, including indirect interaction such as inelastic phonon scattering, the coefficient α in Eq. 1 vanishes, since conduction at each energy within the finite bias window independently obeys the symmetry of linear response and different energies do not mix [11, 12]. Moreover, as discussed recently in Refs. [13, 14], the coefficient α is proportional to the electron interaction strength. This suggests that terms of the form of Eq. 1 can be used to measure interaction strength. As pointed out in Refs. [13, 14], finite \tilde{g} arises from quantum interference and is suppressed by decoherence and thermal averaging.

This Letter presents a detailed study of the symmetry of nonlinear conductance in an open chaotic GaAs quantum dot, using gate-controlled shape distortion to gather ensemble statistics. We focus particular attention on the component of g that is odd in both B and V , as in Eq. 1, at moderately small source-drain voltage,

$V \lesssim \Delta/e$, and fields, $B \lesssim \phi_0/A$, applied perpendicular to the plane of the dot, where Δ is the average quantum level spacing in the dot, $\phi_0 = h/e$ is the flux quantum, and A is the dot area. We find that the component of differential conductance antisymmetric in B , denoted g_{B-} , is also largely antisymmetric in V and shows mesoscopic fluctuations as a function of B , V , and shape-defining gate voltage V_G . As anticipated theoretically [13, 14], we

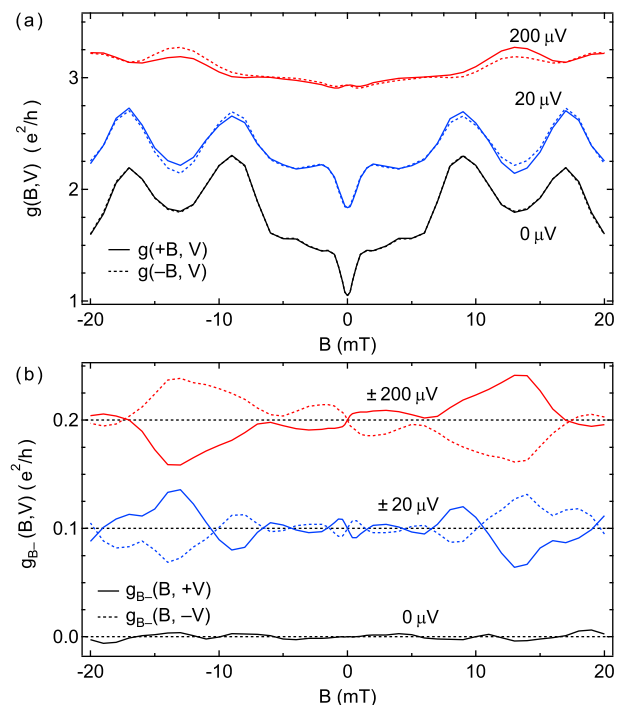


FIG. 1: (a) Differential conductance g for $N = 2$ as a function of magnetic field B (solid curves) and $-B$ (dashed curves) at source-drain bias V as indicated, at base electron temperature $T_{el} = 45$ mK. The blue (red) curves are offset by $+0.5$ ($+1$) e^2/h , respectively. (b) Antisymmetric in B conductance g_{B-} of the traces shown in (a), as a function of B at V (solid curves) and $-V$ (dashed curves) as indicated. The blue (red) curves are offset by $+0.1$ ($+0.2$) e^2/h , respectively. Black curves demonstrate $g(B, V = 0) = g(-B, V = 0)$ and blue/red curves indicate g_{B-} is largely antisymmetric in V .

find that the average coefficient α measured over an ensemble of dot shapes vanishes. The standard deviation of α , denoted $\delta\alpha$, does not vanish and is used to characterize the strength of the interactions, as discussed below. The dependence of $\delta\alpha$ on the number of modes N in the quantum-point-contact leads is found to be in disagreement with theory [13, 14]. However, present theory assumes that electrons do not thermalize within the dot and that decoherence effects are negligible. Accounting for an increased amount of thermalization within the dot at smaller N (consistent with independent measurements of electron distribution functions [15]) appears able to explain qualitatively the observed dependence of $\delta\alpha$ on N .

Measurements were carried out using a quantum dot of area $A \sim 1 \mu\text{m}^2$ formed by Ti/Au depletion gates [see Fig. 2(d)] on the surface of a GaAs/Al_{0.3}Ga_{0.7}As heterostructure 105 nm above the 2D electron gas. A bulk electron density $n \sim 2 \times 10^{11} \text{cm}^{-2}$ and mobility $\mu \sim 2 \times 10^5 \text{cm}^2/\text{Vs}$, giving a mean free path $\ell \sim 1.5 \mu\text{m}$, indicates ballistic transport within the dot. This device contains $N_{dot} \sim 2000$ electrons and has an average level spacing $\Delta = 2\pi\hbar^2/m^*A \sim 7 \mu\text{eV}$, where $m^* = 0.067 m_e$ is the effective electron mass. The dot was designed to lack spatial symmetry [16] and is found to show universal statistics in linear conduction characteristic of chaotic classical dynamics [1, 2, 3]. The gate marked “shape”, with voltage V_G applied, was used to modify the dot boundary, providing a means of generating ensemble statistics [17]. Gates n , $w1$, and $w2$ were actively modulated depending on V_G to maintain an integer number of quantum modes N in each lead throughout the ensemble of shapes. Gates $p1$ and $p2$ were strongly depleted, isolating the adjacent smaller dot, which was used only to measure the electron temperature ($T_{el} = 45 \pm 5 \text{mK}$ at base) using Coulomb blockade peak width.

To measure g , simultaneous lock-in measurements of both differential current and voltage across the dot were made using a four-wire setup at 94.7 Hz with typical ac excitation of $2 \mu\text{V}$, in the presence of a dc source-drain voltage V . All voltages were applied symmetrically across the dot [Fig. 2(a)] to reduce self-gating [16]. The measurement sequence was as follows: $g(B, V, V_G)$ was measured as a function of V (innermost loop) and B (2nd loop, with higher point-density around zero field). Each of these two-parameter sweeps was repeated 20 times to reduce noise (3rd loop), for each of 16 statistically independent shape gate voltages V_G (4th loop). Each multi-parameter sweep, which took about $30 h$ to complete, was measured at $N = 1, 2, 4$ modes in each lead (outermost loop).

As expected for a two terminal device [4, 5, 6], the linear conductance $g(B, V = 0)$ was found to be symmetric in B within measurement resolution, as seen in Fig. 1(a). At finite bias, however, the $\pm B$ symmetry is broken, as seen in the blue and red traces in Fig. 1(a). Decomposing g into components that are symmetric (g_{B+}) and antisymmetric (g_{B-}) in field, $g_{B\pm}(B, V) = (g(B, V) \pm g(-B, V))/2$, we find $g_{B-}(B, V = 0)$ com-

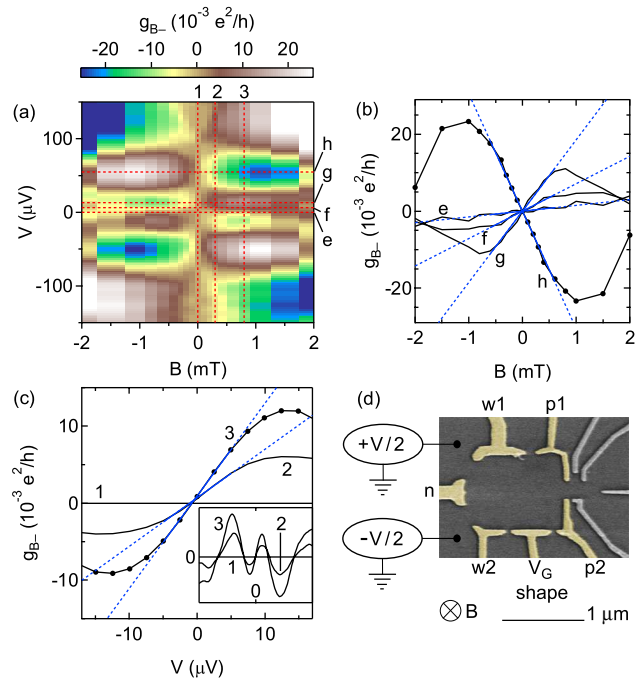


FIG. 2: (a) Antisymmetric component g_{B-} (color scale) as a function of B and V at $N = 2$. Dashed lines indicate cuts shown in (b) and (c). (b) g_{B-} as a function of B at $V = 0, 7.5, 15, 55 \mu\text{V}$. (c) g_{B-} as a function of V at $B = 0, 0.3, 0.8 \text{mT}$. Linear fits to curves in (b) and (c) are shown in dashed blue lines, with solid blue lines indicating the fitting range. Inset to (c) shows the same cuts as in (c) with the V axis extended to $\pm 125 \mu\text{V}$ and the g_{B-} axis extended to $\pm 25 \times 10^{-3} e^2/h$. (d) Electron micrograph of a device with the same gate design as the one measured. Only the yellow gates are used in this experiment. V is applied symmetrically.

parable to the measurement noise of $3 \times 10^{-3} e^2/h$ and barely visible, while at $V = \pm 20 \mu\text{eV}$ and $\pm 200 \mu\text{eV}$, g_{B-} is sizable and is found to be largely antisymmetric in V . The typical amplitude of fluctuations of g_{B-} is $\sim 0.025 e^2/h$, much smaller than the amplitude of fluctuations of g , which is $\sim 0.5 e^2/h$.

The antisymmetry of $g_{B-}(B, V)$ in source-drain voltage V is also seen in Fig. 2(a), which shows $g_{B-}(B, V)$ for $N = 2$ as a two dimensional color plot for a different shape sample than the one shown in Fig. 1. Note that $g_{B-}(B, V)$ changes sign repeatedly as a function of both B and V . Similar characteristics are seen for all dot shapes and values of N , though for some shape samples the antisymmetry in V is more pronounced than in others.

For small fields, $B \lesssim \phi_0/A$, $g_{B-}(B)$ is proportional to B and becomes sizable for $V \gtrsim \Delta/e \sim 7 \mu\text{eV}$, as seen in Fig. 2(b). At larger fields, $B \gtrsim \phi_0/A$, $g_{B-}(B)$ shows mesoscopic fluctuations as a function of B , including sign changes. The field scale where this crossover occurs is consistent with the field scale of weak localization [see Fig. 3(a)] and conductance fluctuations in this device (not shown). This field scale is somewhat smaller than $\phi_0/A \sim 4 \text{mT}$, similar to previous experiments [18, 19] because the relevant area is not the dot area but the area of

typical trajectories before escape, which is larger than A by a factor $\sim \sqrt[3]{N_{dot}}$ [20]. For $V \lesssim \Delta/e$, $g_{B-}(V)$ is also found to be proportional to V and becomes sizable for $B \gtrsim 1$ mT, as seen in Fig. 2(c). For $V \gtrsim \Delta/e$, $g_{B-}(V)$ starts to deviate from the linear dependence on V and shows mesoscopic fluctuations as a function of V , also including sign changes. As mentioned above, while some shapes show more pronounced antisymmetry of g_{B-} with respect to V than others, g_{B-} is predominantly antisymmetric in V , see discussion of Fig. 4(a). The characteristic scales $V \sim \Delta/e$ and $B \sim \phi_0/A$ for mesoscopic fluctuations of $g_{B-}(B, V)$ provide assurance that this component arises from coherent transport within the dot.

The average symmetric component of conductance, $\langle g_{B+} \rangle_{V_G}$, which is maximal around $V = 0$, has a pronounced minimum around $B = 0$ due to ballistic weak localization [21], as seen in Fig. 3(a). From the magnitude of the weak localization feature in $\langle g(B, V = 0) \rangle_{V_G}$, we extract a base-temperature phase coherence time $\tau_\varphi \sim 2$ ns, consistent with previous experiments [21]. As seen in Fig. 3(a), finite V reduces the dip $\langle g(B, V = 0) \rangle_{V_G}$ around $B = 0$, presumably the result of dephasing caused by heating and non-equilibrium effects [22, 23]. Figure 3(b) shows that the standard deviation of the symmetric component δg_{B+} is peaked around $B = 0$, a well-known effect associated with the breaking of time-reversal symmetry [1, 2, 3, 17]. Similar to the weak localization correction, δg_{B+} is also reduced at finite bias. In this case, the reduction is due both to dephasing and an explicit dependence on temperature and energy averaging.

Figure 3(c) shows the shape-averaged antisymmetric component of conductance $\langle g_{B-} \rangle_{V_G}$, which is zero within statistical uncertainty (based on 16 shape samples), indicating that fluctuations of g_{B-} cancel each other upon averaging, as predicted theoretically [13, 14]. As seen in Fig. 3(d), the standard deviation δg_{B-} becomes sizable on a voltage scale of order of the dot level spacing, with a maximum at moderate $|V|$, and then decreases for larger $|V|$, presumably due to heating or decoherence effects. By definition, δg_{B-} is zero for $B = 0$ and, as expected for a g_{B-} that is largely antisymmetric in V , δg_{B-} is comparable to the statistical error along the $V = 0$ line.

To characterize symmetry in terms of statistical quantities, we define normalized symmetry parameters $C_{B\pm V\pm} = \delta^2 g_{B\pm V\pm} / \delta^2 g_{B\pm}$, where $\delta^2 g_{B\pm V\pm}$ is the variance of the component of g with a particular symmetry with respect to B and V . Here, ensemble averaging is performed over the entire (B, V, V_G) parameter space, resulting in approximately $5 \times 4 \times 16$ statistically independent samples. We note that C ranges from zero to one, and $C_{B\pm V\pm} + C_{B\pm V\mp} = 1$. As seen in Fig. 4, $C_{B+V+} \sim 1$ (open squares) and $C_{B+V-} \sim 0$ (filled squares) within the statistical uncertainty, showing that g_{B+} is symmetric in V for all measured conductance samples and modes numbers N . $C_{B-V-} \sim 0.75$ (open circles) and $C_{B-V+} \sim 0.25$ (filled circles) without a strong N dependence, indicating that a significant part of g_{B-}

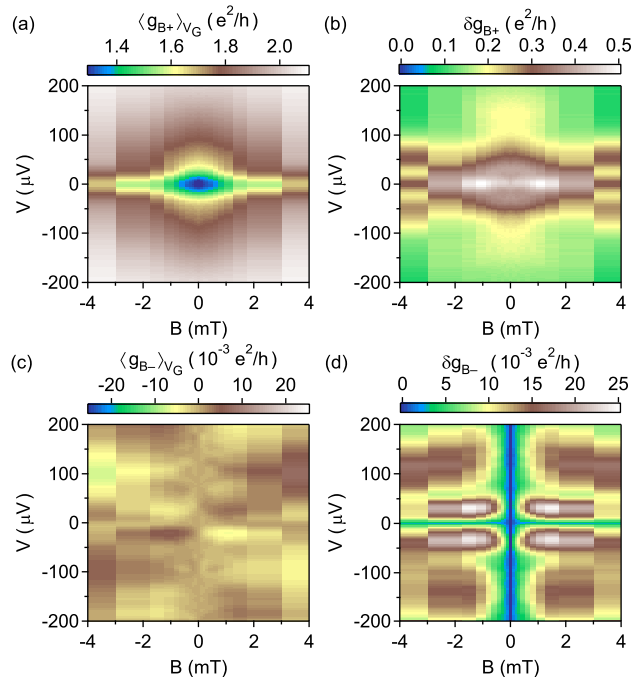


FIG. 3: Average conductance component $\langle g_{B+} \rangle_{V_G}$ (a) and $\langle g_{B-} \rangle_{V_G}$ (c) and standard deviation δg_{B+} (b) and δg_{B-} (d) (color scale) obtained from 16 independent shape samples at $N = 2$ modes as a function of B and V . $\langle g_{B-} \rangle$ is zero within statistical uncertainty; standard deviations are used to characterize the antisymmetries. $\langle g_{B+} \rangle$ shows a strong dip at $(B, V) = 0$ due to ballistic weak localization.

is antisymmetric in V , though the antisymmetry is not perfect.

The interaction coefficient α was extracted for each shape by performing fits linear in both B and V to $g_{B-}(B, V)$ for small $V < \Delta/e$ and $B < \phi_0/A$, similar to the fits shown in Figs. 2(b) and (c). The resulting α is seen to have mesoscopic fluctuations and changes sign frequently, consistent with $\langle \alpha \rangle_{V_G} = 0$ within statistical uncertainty. The standard deviation $\delta\alpha$, used to characterize the strength of electron interaction, is shown in Fig. 4(b) (open triangles) as a function of the mode number N .

For a comparison of the interaction parameter α to theory, we note that Ref. [14] predicts $\delta\alpha$ for $kT \ll N\Delta$, $V \ll \Delta/e$ and $B \ll \phi_0/A$:

$$\delta\alpha = \delta\alpha' \frac{1}{2N^2} \frac{e}{\Delta} \frac{A}{\phi_0} \frac{e^2}{h} \quad (2)$$

where $\delta\alpha'$ is a dimensionless parameter characterizing the electron interaction strength. Using a different approach, Ref. [13] arrives at a similar expression for $\delta\alpha$, with the same dependencies on N and Δ . To facilitate a comparison of experiment and theory, we plot the dimensionless quantity $\delta\alpha'$ in Fig. 4(b), noting a pronounced dependence of $\delta\alpha'$ on N . As defined in Eq. 2, $\delta\alpha'$ is not expected to depend on N , according to Refs. [13, 14]. A

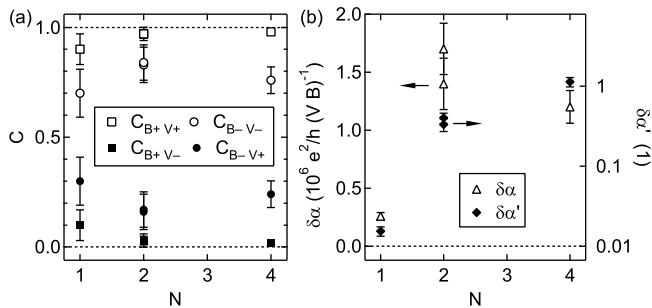


FIG. 4: (a) Normalized symmetry parameter C as a function of the number of modes N for all B and V symmetries as indicated, giving a statistical characterization of the nonlinear field symmetry properties of conductance over all V , B and shape samples measured. (b) Standard deviation $\delta\alpha$ (open triangles) and dimensionless standard deviation $\delta\alpha'$ (solid diamonds) of the interaction parameter (see text) as a function of N .

likely reconciliation is that for $N < 4$, the escape time from the dot is sufficiently long so that electrons have time to equilibrate (thermalize at a higher temperature) before escaping. As a result, $\delta\alpha'$ is reduced at $N = 1, 2$ compared to $N = 4$. Indeed, from direct measurement of electron distribution functions in the same device [15], it is known that for $N = 1$ the distribution of electron energies in the dot is thermal, with an elevated effective temperature that depends on V . For $N = 4$, on the other hand, with a shorter electron dwell time in the dot, non-thermal distributions are seen [15]. For the case $N = 4$, the measured $\delta\alpha' = 1.1 \pm 0.2$ is reasonably consistent

with the theoretical estimate $\delta\alpha' = \pi$ [13], which assumes perfect screening of electrons. Other factors possibly contributing to the observed N dependence of $\delta\alpha'$ may include imperfectly transmitting modes or mode mixing as well as finite temperature and/or decoherence effects, all of which are not currently accounted for theoretically.

In conclusion, we have investigated the magnetic field asymmetry of conductance beyond the linear regime in gate-defined quantum dots. The conductance component g_{B^-} , which is defined to be antisymmetric in B , was found to be also predominantly antisymmetric in V and is of the form of Eq. 1 for $V \ll \Delta/e$ and $B \ll \phi_0/A$. The interaction coefficient α , extracted from linear fits to g_{B^-} , has mesoscopic fluctuations with zero average. Comparison to recent theory [13, 14] is most appropriate for the data with four modes per lead, where electrons remain out of equilibrium during the short dwell time. In this case, consistency with theory [13] relating α to the interaction strength appears reasonable, suggesting good electron screening.

We thank Boris Spivak for suggesting this problem to us and Markus Büttiker and David Sanchez for numerical contributions. This work was supported in part by DARPA under QuIST, ARDA/ARO Quantum Computing Program, and Harvard NSEC. Work at UCSB was supported by QUEST, an NSF Science and Technology Center.

Note added. During completion of this manuscript, closely related experimental work on carbon nanotubes appeared [24].

-
- [1] C. W. J Beenakker, Rev. Mod. Phys. **69**, 731 (1997).
[2] I. L. Aleiner, P. W. Brouwer and L. I. Glazman, Phys. Rep. **358**, 309 (2002).
[3] Y. Alhassid, Rev. Mod. Phys. **72**, 895 (2000).
[4] L. Onsager, Phys. Rev. **38**, 2265 (1931).
[5] H. G. B. Casimir, Rev. Mod. Phys. **17**, 343 (1945).
[6] M. Büttiker, Phys. Rev. Lett. **57**, 1761 (1986).
[7] B. I. Sturman and V. M. Fridkin, *The Photovoltaic and Photorefractive Effects in Non-Centrosymmetric Materials* (Gordon and Breach, New York, 1992).
[8] G. L. J. A. Rikken, J. Fölling and P. Wyder, Phys. Rev. Lett. **87**, 236602 (2001).
[9] E. L. Ivchenko and B. Spivak, Phys. Rev. B **66**, 155404 (2002).
[10] G. L. J. A. Rikken and P. Wyder, Phys. Rev. Lett. **94**, 16601 (2005).
[11] A. Larkin and D. Khmel'nitskii, JETP **91**, 1815 (1986); Phys. Scr. **T14**, 4 (1986).
[12] V. Fal'ko and D. Khmel'nitskii, JETP Lett. **42**, 359 (1989).
[13] D. Sanchez and M. Büttiker, Phys. Rev. Lett. **93**, 106802 (2004); cond-mat/0507292.
[14] B. Spivak and A. Zyuzin, Phys. Rev. Lett. **93**, 226801 (2004);
[15] D. M. Zumbühl *et al.*, (to be published).
[16] A. Löfgren *et al.*, Phys. Rev. Lett. **92**, 46803 (2004).
[17] I. H. Chan *et al.*, Phys. Rev. Lett. **74**, 3876 (1995).
[18] C. M. Marcus *et al.*, Phys. Rev. Lett. **69**, 506 (1992).
[19] D. M. Zumbühl *et al.*, Phys. Rev. B **72**, 81305 (2005).
[20] C. M. Marcus *et al.*, Chaos, Solitons & Fractals **8**, 1261 (1997).
[21] A. G. Huibers *et al.*, Phys. Rev. Lett. **83**, 5090 (1999).
[22] M. Switkes *et al.*, Appl. Phys. Lett. **72**, 471 (1998).
[23] H. Linke *et al.*, Phys. Rev. B **56**, 14936 (1997).
[24] J. Wei *et al.*, cond-mat/0506275.